Journal of Molecular Structure: THEOCHEM 955 (2010) 47–52

Contents lists available at ScienceDirect

Journal of Molecular Structure: THEOCHEM

journal homepage: www.elsevier.com/locate/theochem

An insight into microscopic properties of aprotic ionic liquids: A DFT study

Ali Heidar Pakiari [a,*], Samira Siahrostami [a], Tom Ziegler [b]

[a] Chemistry Department, College of Sciences, Shiraz University, Shiraz, Iran
[b] Department of Chemistry, University of Calgary, 2500 University Drive NW, Calgary, Alta., Canada

ARTICLE INFO

Article history:
Received 25 April 2010
Received in revised form 26 May 2010
Accepted 26 May 2010
Available online 10 June 2010

Keywords:
Aprotic ionic liquid (AIL)
Inter-ionic interaction
ETS–NOCV
Electrostatic interaction
Pauli repulsion
Orbital interaction

ABSTRACT

The relationship between the structure of counter-ions and inter-ionic interaction in ion-pairs is systematically studied for 15 aprotic ionic liquids (AILs) using density functional theory. Five different substituted imidazolium cations and three different polyatomic anions (PA) are taken into account. Theoretical calculations show that the inter-ionic interaction decreases as the vdW volume of the counter-ions increases. By means of a new decomposition scheme called ETS–NOCV [33], which decomposes the total interaction energy into different parts, it can be shown that there is a clear linear relationship between the electrostatic part of the interaction energy and the total interaction energy. Further, for a given PA the electrostatic interaction decreases with increase of the vdW volume of the cation as one would expect. A similar decrease is seen in the electrostatic interaction between a given imidazolium cation on the PAs as the PA vdW volume increases.

1. Introduction

Ionic liquids (IL) represent a new class of solvents with unique characteristics. Due to the presence of a strong anion–cation interaction, they have much higher viscosities, polarities and much lower vapor pressures than those of normal solvents. Their unique solvent properties make them key targets for the development of a large number of emerging technologies, spanning a wide range of applications [1]. For instance, ILs can be exploited as useful solvents for new homogeneous catalytic reactions and other chemical processes with relation to "green chemistry" [2–9].

A wide variety of ionic combinations makes it possible to design ILs with specific properties. They can be classified as aprotic or protic ILs depending on their cation structures. Aprotic ILs (AILs) containing organic cations have low melting points due to the inefficient packing of a large irregular organic cation with a mono atomic or polyatomic inorganic anion [4]. AILs are one of the most important solvent classes in organic chemistry for experimental determination of chemical and physical properties such as melting point, density, viscosity and conductivity [10–14]. The second class is protic ionic liquids (PILs). They are related to the AILs but differ in that the cation has been formed by transferring a proton from a Brønsted acid to a Brønsted base. This class has shown great promise as electrolytes for fuel cells in recent years, because its members can have aqueous solution-like conductivities [15,16].

The study of the relationship between the structures of AILs and their physical properties has been an important theoretical research area in recent years [15,17–20]. There are three extensively used theoretical procedures by which these relationships have been established. (i) The quantitative structure–property relationship (QSPR) can be employed to correlate the melting point with structure [17,18]. (ii) Molecular dynamic simulation is used to compare calculated versus experimental values for some physical properties [19–23]. (iii) Quantum mechanical methods are employed in order to determine interaction energies [24,25], thermodynamic properties [26–29] and also to find a correlation between melting points and interaction energies of ion-pairs [24]. Some AILs have been selected by Dong et al. to inspect the nature of hydrogen bonds between cations and anions [25]. Recently, Fumino et al. have employed density functional theory (DFT) calculations to investigate the role of hydrogen bonding in aprotic and protic ILs [30]. DFT calculations have also been used to investigate intermolecular interactions [31] and to predict vibrational frequencies [32] of some AILs.

In this work, we have performed a systematic theoretical study on five classes of imidazolium-based AILs to determine their inter-ionic interactions by means of DFT. We have made some comparisons among the five classes according to (i) the nature of the polyatomic anion (PA), and (ii) the nature of the cation substitution. Finally, we have used a new scheme based on the Extended Transition State and Natural Orbitals for Chemical Valency (ETS–NOCV

* Corresponding author.
E-mail address: pakiari@shirazu.ac.ir (A.H. Pakiari).

0166-1280/$ - see front matter © 2010 Elsevier B.V. All rights reserved.
doi:10.1016/j.theochem.2010.05.029

[33]) to analyze the relationship between structure and inter-ionic interactions.

2. Computational details

The structure of several anion–cation pairs were optimized using hybrid density functional theory at the B3LYP [34] level of theory in conjunction with a 6-31G(d,p) basis set. Each stationary point was characterized at the same level of theory by computing the vibrational frequencies within the harmonic approximation to make sure that the resulting structures were true minima. The BSSE corrections are considered in all of the steps.

Natural Population Analysis (NPA) [35] of the isolated species (Fig. 1) was carried out, in order to provide initial guesses for different favorable positions for the anions with respect to the cations. For these guesses it was assumed that the interaction between cation and anion is optimal where the most negative sites of the anion are close to the most positive sites of the cation. Therefore, the isolated ion charge analysis was considered in every ion-pair interaction and several structures were optimized before obtaining the optimal one.

The ETS–NOCV decomposition scheme [33], based on the Kohn–Sham approach and the BP86 functional [36,37], was employed to obtain different energy contributions to the total bonding energy. All B3LYP calculations were carried out using GAUSSIAN03 [38] whereas the ETS–NOCV analysis based on BP86 was carried out with ADF [39]. This analysis scheme is not compatible with hybrid functionals. However, the trends in the ion-pair interaction energies are quite similar for BP86 and B3LYP.

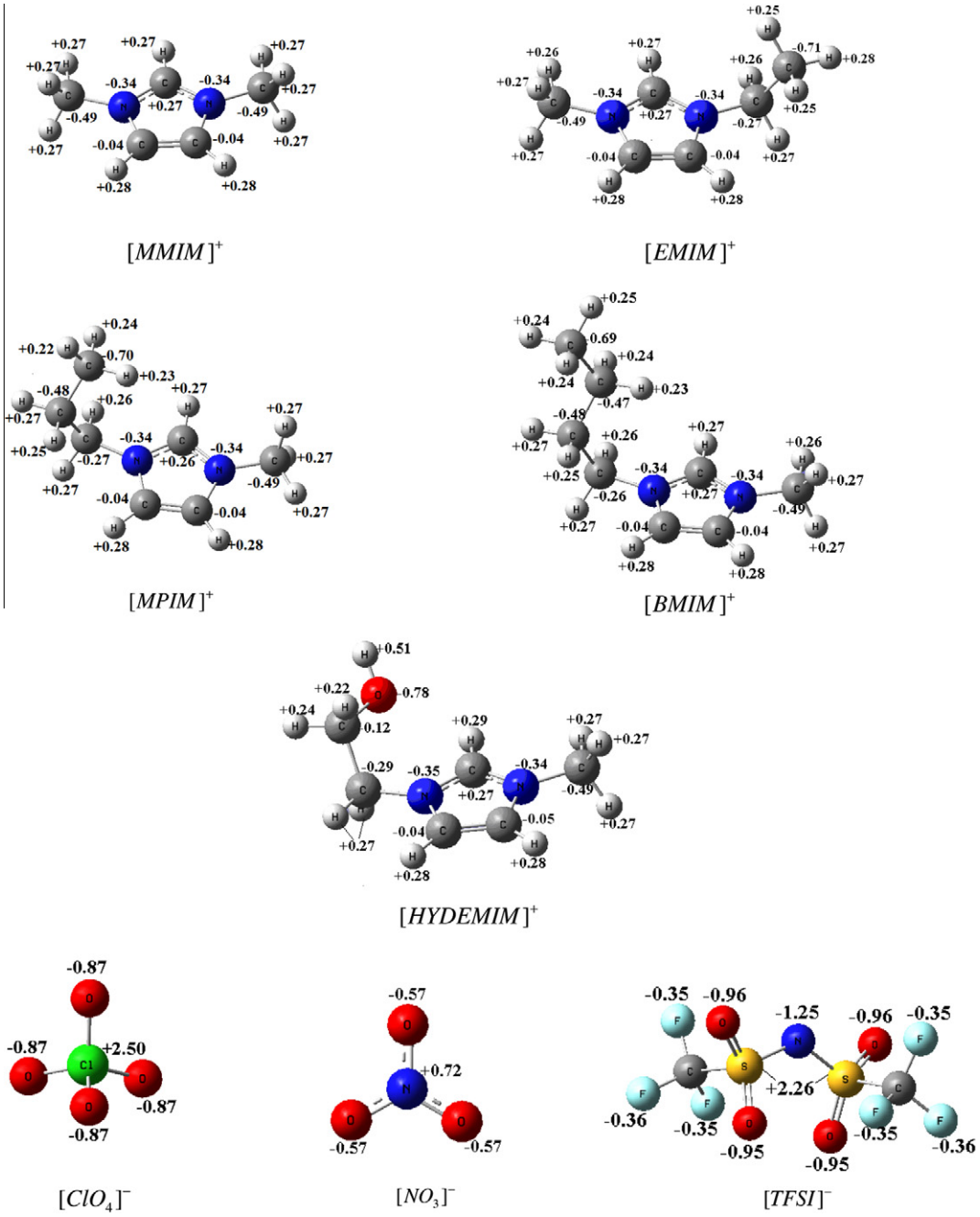

Fig. 1. Optimized structures of selected cations and anions, including their natural atomic charges.

3. Results and discussion

Fifteen AILs have been selected and categorized in five classes with respect to their cation type. The cations are 1,3-dimethylimidazolium $[MMIM]^+$ 1-ethyl-3-methylimidazolium $[EMIM]^+$, 1-methyl-3-propylimidazolium $[MPIM]^+$, 1-butyl-3-methylimidazolium $[BMIM]^+$ and 1-hydroxyethyl-3-methylimidazolium $[HYDEMIM]^+$ for classes I, II, III, IV and V, respectively. The first four cations have been selected to investigate the effect of longer side chains on interaction energies and $[HYDEMIM]^+$ have been considered as an example containing

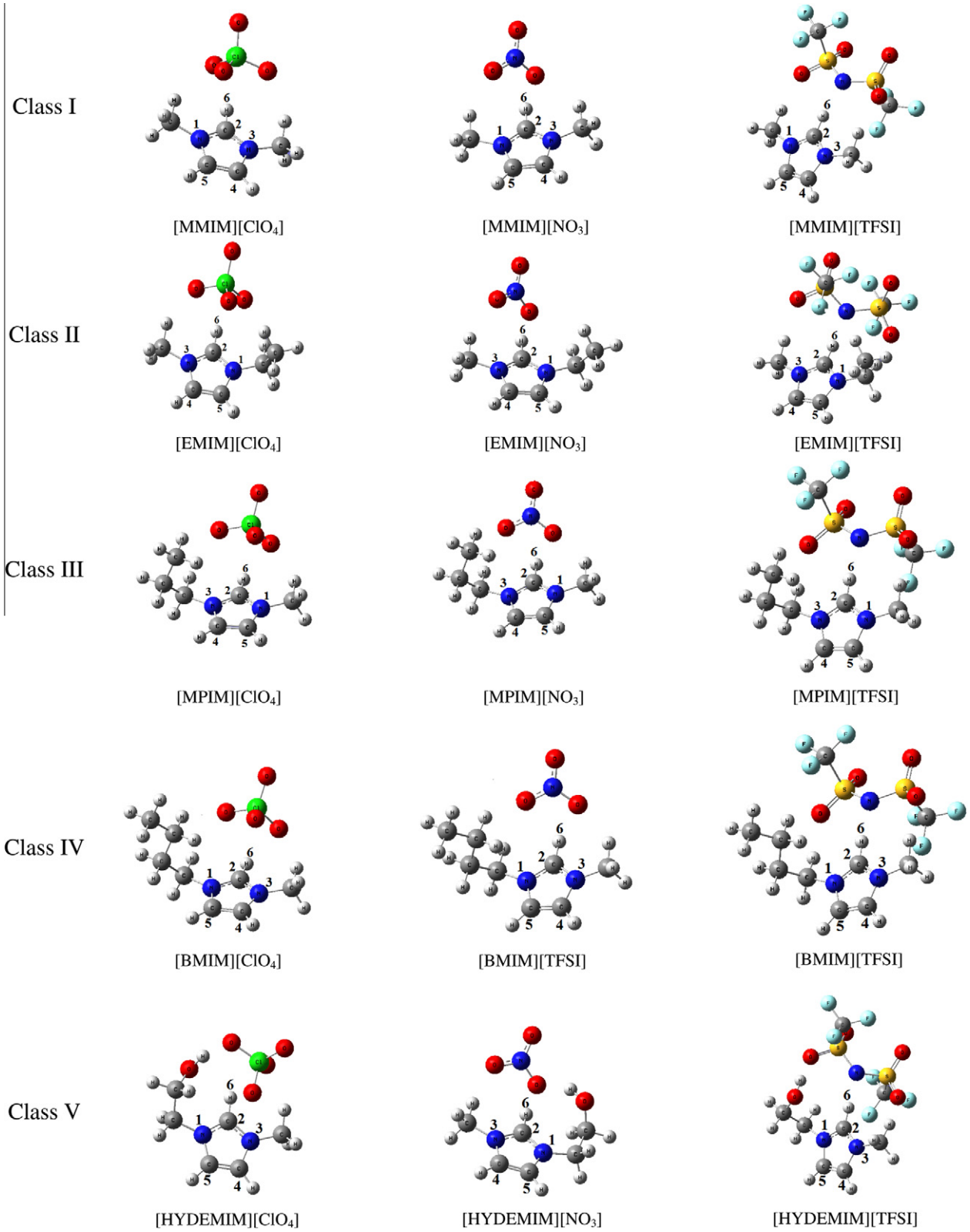

Fig. 2. Optimized structure of 15 different selected AIL. Classes I, II, III, IV and V comprise with $[MMIM]^+$, $[EMIM]^+$, $[MPIM]^+$, $[BMIM]^+$ and $[HYDEMIM]^+$, respectively.

polarized side chains. In order to consider the effect of the PA structure on the interaction energy, three different types of anions have been paired with each cation. In this study the 15 AILs form three series with one anion in each and five different classes with one cation in each. The PAs are perchlorate $[ClO_4]^-$, nitrate $[NO_3]^-$ and bis(trifluoromethanesulfon)imide $[TFSI]^-$ forming series 1–3, respectively. Among these, $[NO_3]^-$ is the smallest and $[TFSI]^-$ is the largest PA. The optimized structures of all AILs are shown in Fig. 2. Details can be found in Supplementary information.

Thermodynamic interaction energies were calculated according to:

$$\Delta\Phi^\circ_{int} = \Phi_{a-c} - (\Phi_a + \Phi_c) \quad (1)$$

where Φ denotes either enthalpy (H) or Gibbs free energy (G). The symbols Φ_{a-c}, Φ_a and Φ_c stand for the ion-pair system, the purely anionic and the cationic species, respectively. The calculated interaction energies are collected in Table 2 for all of the 15 selected AILs. Negative and large values of ΔH°_{int} and ΔG°_{int} (Table 1) are the result of the strong Coulombic anion–cation attraction. There are many factors contributing to the melting point of the AILs and the calculation of isolated ion-pairs is certainly not sufficient to model properties of the condensed phase. Nevertheless, the values of ΔH°_{int} and ΔG°_{int} are in line with the trends in experimental melting point in class II. There are two main trends observed in the calculated data. They will be discussed next.

The calculated interaction enthalpies in absolute terms ($-\Delta H^\circ_{int}$) are depicted versus absolute calculated free energy of interaction ($-\Delta G^\circ_{int}$), for all 15 systems in Fig. 3. There are three main series in this figure corresponding to the three selected anions (three series). As it is observed, there is the following trend for the absolute interaction energies among the AILs of each class $[\cdots][NO_3] > [\cdots][BF_4] > [\cdots][TFSI]$, where $[\cdots]$ can be each of the five selected cations. Within a class the inter-ionic interaction energy decreases with increasing volume of the PA. For the class V one hydrogen atom of the ethyl side chain is replaced by hydroxyl thus creating a polarized alkyl side chain. Comparing classes II and V, it is observed that polarized alkyl side chains increase the interaction energy.

Table 1
Summary of experimental data (relevant references are indicated next to compound names) and theoretical data (B3LYP level of computation including BSSE corrections has been used).

Salt name	ΔH°_{int} (kJ mol^{-1})	ΔG°_{int} (kJ mol^{-1})	Melting point (°C ± 3)
Class I			
[MMIM][NO_3]	−384.4	−342.4	N.O.[c]
[MMIM][ClO_4]	−342.0	−304.3	N.O.
[MMIM][TFSI]	−323.4	−276.2	N.O.
Class II			
[EMIM][NO_3][a]	−379.6	−340.2	75
[EMIM][ClO_4][a]	−338.3	−298.2	7
[EMIM][TFSI][a]	−322.7	−273.9	−19
Class III			
[MPIM][NO_3]	−376.0	−337.0	N.O.
[MPIM][ClO_4]	−334.1	−297.8	N.O.
[MPIM][TFSI]	−316.6	−270.1	N.O.
Class IV			
[BMIM][NO_3]	−375.9	−332.2	N.O.
[BMIM][ClO_4]	−333.8	−292.6	N.O.
[BMIM][TFSI][b]	−316.3	−254.8	−5
Class V			
[HYDEMIM][NO_3]	−387.7	−341.2	N.O.
[HYDEMIM][ClO_4]	−352.4	−307.1	N.O.
[HYDEMIM][TFSI]	−328.0	−276.2	N.O.

[a] Ref. [13].
[b] Ref. [29].
[c] Not observed.

Table 2
The results of ETS–NOCV analysis based on BP86 functional for the 15 selected AILs.

Salt name	ΔE_{Pauli} (kJ mol^{-1})	ΔE_{elstat} (kJ mol^{-1})	ΔE_{orb} (kJ mol^{-1})	ΔE_{int} (kJ mol^{-1})
Class I				
[MMIM][NO_3]	149.1	−423.5	−114.1	−388.6
[MMIM][ClO_4]	89.9	−375.5	−64.8	−350.3
[MMIM][TFSI]	107.4	−346.2	−77.9	−316.7
Class II				
[EMIM][NO_3]	148.8	−417.8	−114.7	−383.7
[EMIM][ClO_4]	97.0	−375.0	−71.1	−349.2
[EMIM][TFSI]	109.8	−346.6	−78.9	−315.6
Class III				
[MPIM][NO_3]	148.1	−414.7	−115.1	−381.7
[MPIM][ClO_4]	90.7	−367.7	−65.4	−342.4
[MPIM][TFSI]	108.5	−340.9	−76.6	−309.0
Class IV				
[BMIM][NO_3]	149.0	−411.3	−115.9	−378.2
[BMIM][ClO_4]	90.8	−363.5	−66.0	−338.7
[BMIM][TFSI]	109.1	−339.1	−77.4	−307.4
Class V				
[HYDEMIM][NO_3]	184.3	−468.9	−142.4	−427.0
[HYDEMIM][ClO_4]	119.5	−406.8	−84.2	−371.6
[HYDEMIM][TFSI]	119.4	−369.3	−88.1	−338.0

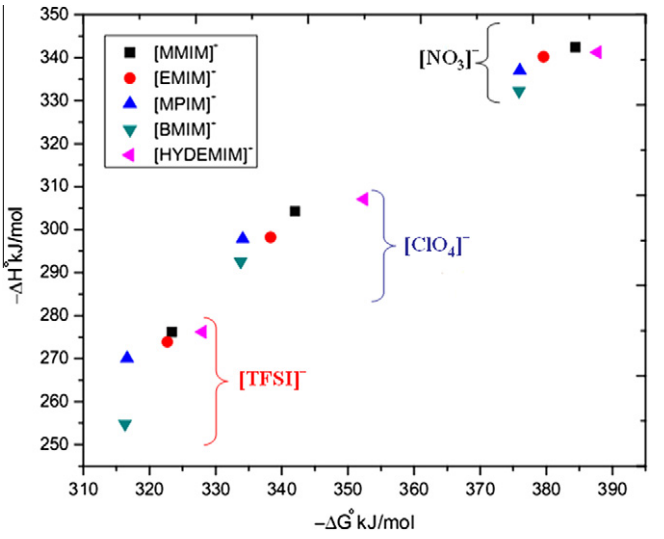

Fig. 3. Calculated interaction enthalpies in absolute terms ($-\Delta H^\circ_{int}$) vs. absolute calculated free energies of interaction ($-\Delta G^\circ_{int}$). The three series are related to the same anions.

We shall now analyze the ion-pair interaction in more details. The analysis will be based on the ETS–NOCV scheme [33]. For technical reasons we are not able to use B3LYP but must instead resort to the pure functional BP86. The electronic interaction energy (enthalpy) ΔE_{int} calculated by BP86 is however similar to that found by B3LYP, especially with regard to the trends among different ion-pairs. We note, however, that the quantitative numbers we want to report are the ΔH°_{int} and ΔG°_{int} values in Table 1 based on B3LYP. Our BP86 and ETS–NOCV results are just used to analyze the trends in the calculated B3LYP results of Table 1.

3.1. ETS–NOCV analysis

The ETS–NOCV [33] scheme combines the Extended Transition State method (ETS) [40] and Natural Orbitals for Chemical Valance (NOCV) [41]. It is based on the Kohn–Sham approach and decomposes the interaction energy of the molecule *AB*, formed from the

two different fragments A° and B°, into a number of chemically meaningful components [33]:

$$E_{AB} - E_A^\circ - E_B^\circ = \Delta E_{int} = \Delta E_{prep} + \Delta E_{elstat} + \Delta E_{Pauli} + \Delta E_{orb} \quad (2)$$

where ΔE_{prep} is the energy required for the distortion of two fragments A° and B° from their equilibrium geometries to their final structures in AB. The second and third terms are the electrostatic ion-pair interaction and the Pauli ion-pair repulsion contributions, respectively. Together they are called the steric interaction energy between the two ion-pairs:

$$\Delta E_{steric} = \Delta E_{Pauli} + \Delta E_{elstat} \quad (3)$$

The last term in Eq. (2), ΔE_{orb}, is the orbital interaction, representing the interaction between occupied molecular orbitals on one fragment and unoccupied molecular orbitals of the other fragment. It also represents the mixing of occupied and virtual orbitals within the same fragment [33].

The result of the ETS–NOCV analysis has been reported in Table 2 for all of the 15 selected AILs. Consistent with the B3LYP calculations, the maximum interaction energy in absolute terms ($-\Delta E_{int}$) for each class is found for $[\cdots][NO_3]$. On the other hand, for a series of AILs with the same anions but different cations the absolute values of $-\Delta E_{int}$ is decreasing as the length of the alkyl side chain increases. Comparing classes II and V, it is observed that $-\Delta E_{int}$ increase in class V. These observations, which are in agreement with the results of Table 1, can be explained by looking at the electrostatic component of the interaction energy. In Fig. 4 the $-\Delta E_{int}$ values are depicted vs. $-\Delta E_{elstat}$ for the AILs of each class. Similar to the trends found in Fig. 3, there are three areas corresponding to three selected anions. As it is observed, there are good agreements between the electrostatic part and the total interaction energy in the case of either the AILs of each class or the AILs of each series. The electrostatic interaction is inversely proportional to the sum of the radii of the two counter-ions:

$$\Delta E_{elstat} \propto -\frac{1}{R_a + R_c} \quad (4)$$

where R_a and R_c are the anion and the cation radii, respectively that can be obtained through volume calculations of each individual ion as:

$$V = \frac{4}{3}\pi R^3 \quad (5)$$

These calculated $R_a + R_c$ values are reported in Table 3 and the electrostatic interactions have been depicted in terms of the inverse sum $(R_a + R_c)^{-1}$ in Fig. 5. As it can be observed, there is a clear relationship between $-\Delta E_{elstat}$ and $(R_a + R_c)^{-1}$ for the AILs having either the same anion or the same cation, as expected from Eq. (4). It clarifies why those AILs having either anions or cations with large vdW volumes show diminished electrostatic interactions. This is to be expected from a model of two touching and interacting spheres of uniform and opposite charge interacting with each other. The $[NO_3]^-$ anion is planar and has a smaller vdW volume than the two other anions and it should be expected to pack more closely to the cation than the other anions. On the other hand, $[TFSI]^-$, the largest anion, has the weakest interaction with the cation. The net result of these factors is that we find the formation of the strongest and the weakest anion–cation interaction in the case of AILs containing $[NO_3]^-$ and $[TFSI]^-$, respectively, in each class (Fig. 4). There is the same argument for the electrostatic interaction of the cations with different vdW volume in each series (Fig. 4).

Table 3
The calculated sum of radii of the 15 selected AILs.

Salt name	$R_c + R_a$ (Å)	$-1/R_c + R_a$ (1/Å)
Class I		
[MMIM][NO_3]	6.740	−0.148
[MMIM][ClO_4]	7.240	−0.138
[MMIM][TFSI]	8.100	−0.123
Class II		
[EMIM][NO_3]	7.110	−0.141
[EMIM][ClO_4]	7.610	−0.131
[EMIM][TFSI]	8.470	−0.118
Class III		
[MPIM][NO_3]	7.440	−0.134
[MPIM][ClO_4]	7.940	−0.126
[MPIM][TFSI]	8.800	−0.114
Class IV		
[BMIM][NO_3]	7.820	−0.128
[BMIM][ClO_4]	8.320	−0.120
[BMIM][TFSI]	9.180	−0.109
Class V		
[HYDEMIM][NO_3]	7.110	−0.141
[HYDEMIM][ClO_4]	7.610	−0.131
[HYDEMIM][TFSI]	8.470	−0.118

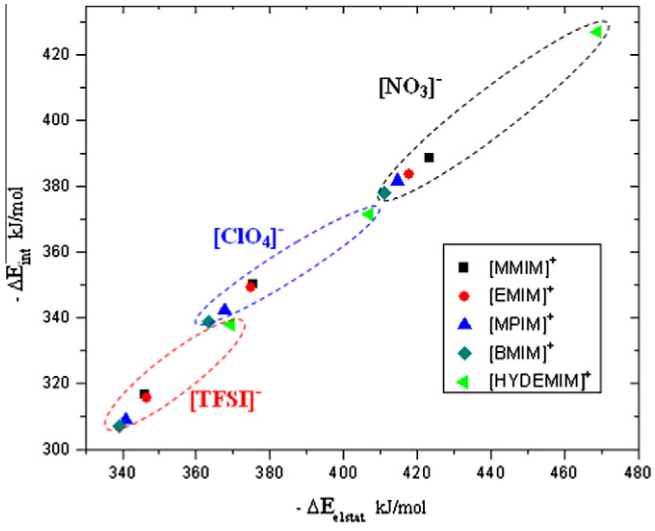

Fig. 4. Calculated interaction energies in absolute terms ($-\Delta E_{int}$) vs. absolute calculated electrostatic interaction ($-\Delta E_{elstat}$) for the classes of the AILs containing the same cation but different anions. There are three series related to the AILs with the same anions.

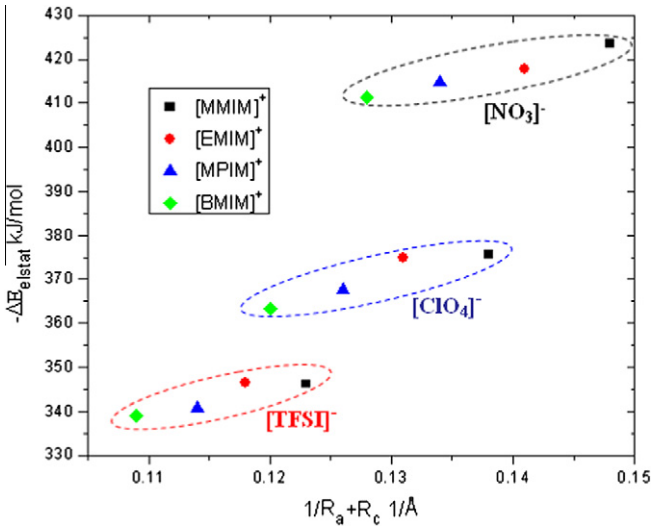

Fig. 5. Calculated electrostatic interactions in absolute terms ($-\Delta E_{elstat}$) vs. calculated radii of counter-ions for the classes of the AILs containing the same cation but different anions. There are three series related to the AILs with the same anions.

In the case of AILs of the class V, the calculated radii of the counter-ions are the same as those of class II. Although there is a linear relationship between $-\Delta E_{elstat}$ and $(R_a + R_c)^{-1}$ in this class, we did not include it in the Fig. 5 for the following reason. In this case, beside of the vdW volume of the counter-ions, there is a strong hydrogen bonding between OH of hydroxyethyl substitution and PA, affecting the magnitude of the electrostatic interaction and the total interaction energy.

4. Conclusion

We have performed a systematic theoretical study on five classes of imidazolium-based AILs to calculate their inter-ionic interactions. By means of the new ETS–NOCV analysis scheme, it can be shown quantitatively that the total interaction energy of AILs is directly governed by the electrostatic interaction between the ion-pairs. Those AILs with either the largest anion or cation give the weakest interaction energy within a given of counter-ion, due to a longer radius and a weaker electrostatic attraction. Although the class of AILs with the polarized alkyl side chain ([HYDEMIM][···]) for each member have the same sum $R_a + R_c$ as the corresponding members [EMIM][···], they always display a stronger total interaction energy than their nonpolarized analogues ([EMIM][···]) due to the hydrogen bonding via OH with polyatomic anions which affects strongly the amount of electrostatic interaction.

Acknowledgment

The authors gratefully acknowledge generous allocation of computing time from University of Calgary for Advanced Computing.

Appendix A. Supplementary data

Supplementary data associated with this article can be found, in the online version, at doi:10.1016/j.theochem.2010.05.029.

References

[1] M. Armand, F. Endres, D.R. MacFarlane, H. Ohno, B. Scrosati, Nat. Mater. 8 (2009) 621.
[2] S. Fujita, H. Kanamaru, H. Senboku, M. Arai, Int. J. Mol. Sci. 7 (2006) 438.
[3] T. Nishida, Y. Tashiro, M. Yamamoto, J. Fluorine Chem. 120 (2003) 135.
[4] O. Hiroyuki, Electrochemical Aspects of Ionic Liquids, Wiley, New York, 2005.
[5] D. Strasser, F. Goulay, M.S. Kelkar, E.J. Maginn, S.R. Leone, J. Phys. Chem. A 111 (2007) 3191.
[6] M. Ue, M. Takeda, A. Toriumi, A. Kominato, R. Hagiwara, Y. Ito, J. Electrochem. Soc. 150 (2003) 499.
[7] J.D. Stenger-Smith, C.K. Webber, N. Anderson, A.P. Chafin, K. Zong, R. Reynolds, J. Electrochem. Soc. 149 (2002) A973.
[8] A. Lewandowski, A. Swiderska, Solid State Ionics 161 (2003) 243.
[9] S. Washiro, M. Yoshizawa, H. Nakajima, H. Ohno, Polymer 45 (2004) 1577.
[10] J.Z. Yang, P. Tian, L.L. He, W.G. Xu, Fluid Phase Equilib. 204 (2003) 295.
[11] H. Ohno, M. Yoshizawa, Solid State Ionics 154–155 (2002) 303.
[12] S. Seki, K. Hayamizu, S. Tsuzuki, K. Fujii, Y. Umebayashi, T. Mitsugi, T. Kobayashi, Y. Ohno, Y. Kobayashi, Y. Mita, H. Miyashiroa, S. Ishigurod, Phys. Chem. Chem. Phys. 11 (2009) 3509.
[13] J. Palomar, V.R. Ferro, J.S. Torrecilla, F. Rodríguez, Ind. Eng. Chem. Res. 46 (2007) 6041.
[14] Y.U. Paulechk, G.J. Kabo, A.V. Blokhin, A.S. Shaplov, E.I. Lozinskaya, Ya.S. Vygodskii, J. Chem. Thermodyn. 39 (2007) 158.
[15] M. Ue, J. Electrochem. Soc. 141 (1994) 3336.
[16] H. Markusson, J.P. Belieres, P. Johansson, C.A. Angell, P. Jacobsson, J. Phys. Chem. A 111 (2007) 8717.
[17] J.K. Shah, J.F. Brennecke, E.J. Maginn, Green Chem. 4 (2002) 112.
[18] S. Trohalaki, R. Pachter, G.W. Drake, T. Hawkins, Energy Fuels 19 (2005) 279.
[19] A.R. Porter, S.Y. Liem, P.L.A. Popelier, Phys. Chem. Chem. Phys. 10 (2008) 4240.
[20] G. Raabi, J. Kohler, J. Chem. Phys. 128 (2008) 1545091.
[21] R. Hagiwara, Y. Ito, J. Fluorine Chem. 105 (2000) 221.
[22] N. Sun, X. He, K. Dong, X. Zhang, X. Lu, H. He, S. Zhang, Fluid Phase Equilib. 246 (2006) 137.
[23] Z. Meng, A. Dolle, W.R. Carper, J. Mol. Struct. (THEOCHEM) 585 (2002) 119.
[24] E.A. Turner, C.C. Pye, R.D. Singer, J. Phys. Chem. A 107 (2003) 2277.
[25] K. Dong, S. Zhang, D. Wang, X. Yao, J. Phys. Chem. A 110 (2006) 9775.
[26] Y. Wang, H. Li, S. Han, J. Phys. Chem. B 110 (2006) 24646.
[27] Y. Guangren, S. Zhang, Fluid Phase Equilib. 255 (2007) 86.
[28] V.N. Emel'yanenko, S.P. Vervkin, A. Heintz, J. Am. Chem. Soc. 129 (2007) 3930.
[29] I. Krossing, J.M. Slattery, C. Daguenet, P.J. Dyson, A. Oleinikova, H. Weingartner, J. Am. Chem. Soc. 128 (2006) 13427.
[30] K. Fumino, A. Wulf, R. Ludwig, Phys. Chem. Chem. Phys. 11 (2009) 8790.
[31] H. Shirota, J.F. Wishart, E.W. Castner Jr., J. Phys. Chem. B 111 (2007) 4819.
[32] E.R. Talaty, S. Raja, V.J. Storhaug, A. Dolle, W.R. Carper, J. Phys. Chem. B 108 (2004) 13177.
[33] M.P. Mitoraj, A. Michalak, T. Ziegler, J. Chem. Theory Comput. 5 (2009) 962.
[34] P.J. Stephens, F.J. Devlin, C.F. Chabalowski, M.J. Frisch, J. Phys. Chem. 98 (1994) 11623.
[35] A.E. Reed, L.A. Curtiss, F. Weinhold, Chem. Rev. 88 (1988) 899.
[36] A. Becke, Phys. Rev. A 38 (1988) 3098.
[37] J.P. Perdew, Phys. Rev. B 34 (1986) 7406.
[38] M.J. Frisch et al., GAUSSIAN 03, Revision B.03, Gaussian, Inc., Pittsburgh, PA, 2003.
[39] G. te Velde, F.M. Bickelhaupt, E.J. Baerends, C. Fonseca Guerra, S.J.A. van Gisbergen, J.G. Snijders, T. Ziegler, J. Comput. Chem. 22 (2001) 931. and references therein.
[40] T. Ziegler, A. Rauk, Theor. Chim. Acta 46 (1977) 1.
[41] A. Michalak, M. Mitoraj, T. Ziegler, J. Phys. Chem. A 112 (2008) 1933.